POLARIZATION MEASUREMENTS OF POST–ASYMPTOTIC GIANT BRANCH CANDIDATES AND RELATED STARS

M. Parthasarathy and S. K. Jain[1]

Indian Institute of Astrophysics, Koramangala, Bangalore 560034, India; partha@iiap.res.in

and

G. Sarkar[2]

Inter-University Centre for Astronomy and Astrophysics, Post Bag 4, Ganeshkhind, Pune 411007, India; gsarkar@iucaa.ernet.in

ABSTRACT

We have obtained *UBVRI* polarization measurements of 26 post–asymptotic giant branch (post-AGB) candidates and related stars. The extremely metal-poor post-AGB star HR 4049 has been observed several times. In most cases we find the objects to be intrinsically polarized. The polarization measurements presented in this paper indicate asymmetric circumstellar dust shells and disks around these stars. For some objects the steep percent polarization λ-dependence and large degree of polarization suggest that scattering by circumstellar dust grains may be responsible for the observed polarizations in the blue.

Key words: circumstellar matter — infrared: stars — polarization — stars: AGB and post-AGB — stars: evolution

1. INTRODUCTION

From an analysis of *IRAS* data, several cooler and hotter post–asymptotic giant branch (post-AGB) stars and proto–planetary nebulae (PPNe) have been discovered (Parthasarathy & Pottasch 1986; Pottasch & Parthasarathy 1988; Hrivnak et al. 1989; Kwok 1993; Parthasarathy et al. 2000), indicating an evolutionary sequence in the transition region from the tip of the AGB to planetary nebulae (PNe). Polarization characteristics of stars in the stages of evolution from a red giant to a planetary nebula were investigated by Johnson & Jones (1991). Polarization was found to be characteristic of the majority of these stars. They found that the maximum observed polarization increases with age as the star evolves up the AGB to the PPN phase, in which the polarization reaches a maximum. The polarization then decreases as the star further evolves into a PN. Trammell et al. (1994) and Parthasarathy & Jain (1993) presented polarimetry of several post-AGB stars. These studies indicated that aspherical morphology shells seem to be a common feature, and they may originate during the AGB mass-loss phase.

Ueta et al. (2000) imaged 27 PPNe using the *Hubble Space Telescope* (*HST*) WFPC2. If one combines the *HST* imaging results of 44 PPNe (Meixner 2000; Ueta et al. 2000), 80% of the 44 PPNe have resolvable optical reflection nebulosities, and all of them are axisymmetric. Gledhill et al. (2001) carried out imaging polarimetry to detect and image the dusty circumstellar envelopes of a sample of PPNe/post-AGB stars at near-IR wavelengths. They have suggested that the range of observed envelope morphologies results from the development of an axisymmetric dust distribution during the superwind phase at the end of the AGB. They found that the observed polarization in PPNe can be explained in terms of scattering in a disk/envelope geometry viewed at various inclinations. However, Ueta et al. (2004, 2005) suggest that differences in morphology between bipolar reflec-

tion nebulae and elliptical nebulae are due primarily to differences in optical depth and that the effect of inclination is only secondary. They found that equatorial enhancement of circumstellar shells in some optically thin PPNe comes with various degrees of contrast. *HST* imaging results of PPNe (Ueta et al. 2000) show that most of the PPNe have a basic bipolar structure. The differences in appearance then arise from the orientation, density distribution, and asymmetry of the circumstellar envelopes.

To understand the polarization characteristics of post-AGB stars, we carried out *UBVRI* linear polarization measurements of 26 post-AGB candidates and related stars (Table 1), presented in this paper. Our observations are a bit old, and since our observations, several new results and data on these stars have been reported based on *HST* images, mid-IR imaging, imaging polarimetry, etc. (see, e.g., Gledhill et al. 2001; Meixner et al. 1997; Ueta et al. 2000, 2001, 2004, 2005). However, since many post-AGB stars are found to be variable, we believe that our observations, although old, would add to the database and would be useful in understanding the evolution of these stars. Our data would be useful to others who will carry out further polarimetric observations of these stars. In § 3.2 we compare the observations of post-AGB stars from our sample with available *HST*, mid-IR images and ground-based imaging polarimetric observations.

2. OBSERVATIONS

UBVRI polarization observations were made with a star and sky chopping polarimeter (Jain & Srinivasulu 1991) coupled at the f/13 Cassegrain focus of the 1 m telescope at the Vainu Bappu Observatory, Kavalur, Indian Institute of Astrophysics. The details of the instrument and the method of data reduction have been described by Jain & Srinivasulu (1991). A dry ice–cooled EMI 9658-R (extended S-20) photomultiplier tube and Fernie (1974) combination of *UBVRI* broadband glass filters were used. The average instrumental polarization, determined every night by observing several unpolarized standard stars (Serkowski et al. 1975), was found to be $P = 0.1\%$. It was subtracted vectorially from the measured polarization of the program stars. The zero of the position angles was determined by observing polarized

---

TABLE 1
Observed Post-AGB Candidates and Related Stars

| IRAS | Name | l (deg) | b (deg) | V (mag) | Spectral Type | IRAS Fluxes[a] (Jy) | | | | E(B − V) (Interstellar) |
						12 μm	25 μm	60 μm	100 μm	
00047+0637	HD 231	103.81	−54.34	7.45	A5	1.19	0.74	0.40L	1.00L	0.081
05040+4820	SAO 40039	159.75	+4.76	9.65	A4 I	0.25L	7.20	20.20	11.00	. . .
06338+5333	HD 46703	161.98	+19.59	9.09	F7 I	0.46	0.38:	0.40L	1.15L	0.085
07008+1050	HD 52961	204.67	+7.57	7.38	A0	4.53	2.22	0.95	0.87:	0.099
07134+1005	HD 56126	206.75	+9.99	8.27	F5 Iab	24.51	116.70	50.13	18.72	0.080
07331+0021	AI CMi	217.80	+9.95	8.31	G5 Iab	15.32	68.11	18.51	3.68	0.081
07559−5859	HD 65750	272.25	−15.24	6.25	M0−3 II	101.50	43.88	54.19	103.00	0.276
10158−2844	HD 89353 (HR 4049)	266.85	+22.93	5.53	B9.5 Ib	48.25	9.55	1.77	1.69L	0.065
10215−5916	HD 302821	285.14	−1.88	9.05	K0	200.80	1755.0	851.80	181.10	. . .
11000−6153................	HD 95767	290.54	−1.95	8.88	F3 II	22.13	15.65	10.90	58.88	. . .
11331−1418................	HD 100764	276.86	+44.41	8.73	C	7.81	10.19	9.16	6.12	0.040
11385−5517................	HD 101584	293.03	+5.94	7.02	F0 Iape	92.60	138.30	193.00	104.00	0.373
12175−5338	SAO 239853	298.30	+8.67	9.36	A7 I	1.03	20.59	7.57	2.52	0.196
12222−4652	HD 108015	298.25	+15.48	7.98	F5 Ib	32.46	33.23	7.99	2.41	0.115
12538−2611................	HR 4912	304.34	+36.40	6.62	F3 Ia	1.24	1.59	0.55	1.00L	0.079
15039−4806	HD 133656	325.04	+8.65	7.51	A2 Ib	0.25L	4.29	3.61	7.98L	0.301
16206−5956	SAO 243756	326.77	−7.49	9.79	A3 Iab	0.36L	11.04	12.30	4.83	0.217
17436+5003	HD 161796	77.13	+30.87	7.12	F3 Ib	6.12	183.50	151.70	48.67	0.030
17534+2603	HD 163506	51.43	+23.19	5.46	F2 Ibe	97.52	54.49	13.42	6.04	0.090
18095+2704		53.84	+20.18	10.4	F3 Ib	45.09	125.70	27.83	5.64	0.099
18184−1623	HD 168625	14.98	−0.96	8.44	A I	69.97	325.40	116.90:	583.70L	. . .
19114+0002	HD 179821	35.62	−4.96	8.12	G5 Ia	31.33	648.30	515.90	168.10	. . .
19486+1350	HD 353895 (TW Aql)	52.24	−6.42	9.9	K7 I	0.27L	5.23	11.25	3.48	0.281
19500−1709	HD 187885	23.98	−21.04	8.68	F3 Iab	27.82	165.00	73.40	18.18	0.205
20004+2955	HD 333385	67.43	−0.36	8.71	G7 Ia	31.72	36.96	4.66	33.47L	. . .
22272+5435	HD 235858	103.35	−2.52	8.87	G5 I	73.88	302.40	96.59	40.97	. . .

[a] A colon indicates a moderate-quality IRAS flux measurement; L indicates an upper limit.

standard stars (Hsu & Breger 1982). Details of the program stars are given in Table 1.

3. ANALYSIS

The measured percentage polarizations (P) and position angles (θ) along with the Julian Dates of observation are given in Table 2. In the case of the very metal-poor post-AGB star HR 4049 (IRAS 10158−2844; HD 89353), we observed it on several occasions to study the variations in P and θ. The polarization measurements of HR 4049 are listed in Table 3.

In Figure 1 we show the variation of polarization and position angle with wavelength for the stars given in Table 2. The observed polarization values given in Table 2 have not been corrected for interstellar polarization. Interstellar polarization follows a Serkowski law, which is a smoothly varying function of wavelength with a small slope in the optical (Wilking et al. 1980), and is constant with time. For some of the stars (Table 2), Trammell et al. (1994) estimated the interstellar polarization (see Table 2 in Trammell et al. 1994).

3.1. Notes on Stars Whose Evolutionary Status Is Not Clear

Most stars in Table 1 are in the post-AGB phase of evolution (see the reviews by Kwok 1993; van Winckel 2003 and references therein). However, some objects whose evolutionary status is not clear and that may be related to the post-AGB phase were also observed.

IRAS 00047+0637 (HD 231).—Its near-IR colors are similar to that of a normal A star of B − V = 0.18 and E(B − V) = 0.03 (Whitelock et al. 1989). It may be a "Vega-like star" or a post-AGB star.

IRAS 07559−5859 (HD 65750).—This is a unique dusty variable M0−3 II star (Chiar et al. 1993 and references therein) embedded in the bipolar reflection nebula IC 2220. It may be in rapid evolution to the AGB.

IRAS 10215−5916 (CPD −58°2154).—This is a binary system (Molster et al. 1999). The hotter component of the binary system may be a post-AGB star (Sivarani et al. 2001).

IRAS 11331−1418 (HD 100764).—This is a warm carbon star (early R star) with a detached cold dust shell (Parthasarathy 1991). Modeling of its circumstellar dust (Skinner 1994) revealed that the star must have a massive dusty disk. The dusty disk may have been acquired from a binary companion that has evolved through the AGB and PN phases.

IRAS 18184−1623 (HD 168625).—This has variously been classified as a post-AGB candidate (Parthasarathy 1989), a luminous blue variable (LBV) (Hutsemekers et al. 1994), and a variable hypergiant or a marginally dormant LBV (Sterken et al. 1999). Our polarization measurements indicate variable intrinsic polarization. Gledhill et al. (2001) obtained J-band polarimetric observations. They found the polarization pattern to be unusual, consisting of almost parallel vectors oriented at a position angle of approximately 20°. The polarized flux image was pointlike and coincident with the peak in total flux. They speculated a bipolar geometry for which the bipolar structure is not resolved. Robberto & Herbst (1998) suggested that the emission results from "a relatively thin edge-brightened shell." They found that at mid-IR wavelengths, most of the flux comes from an extended (12″ × 16″) elliptical nebula with two well-defined peaks. A similar morphology was seen by Meixner et al. (1999). Recently, O'Hara et al. (2003) imaged the dust ring around HD 168625 with NICMOS on board the *HST*. They found a detached dust

		U		B		V		R		I	
	DATE	*P*	*θ*	*P*	*θ*	*P*	*θ*	*P*	*θ*	*P*	*θ*
OBJECT	(JD)	(%)	(deg)	(%)	(deg)	(%)	(deg)	(%)	(deg)	(%)	(deg)
IRAS 00047+0637 (HD 231)	2,447,918			0.40 ± 0.06	123.5 ± 4.3	1.01 ± 0.05	95.2 ± 1.4	0.54 ± 0.05	86.2 ± 2.5	0.54 ± 0.10	92.0 ± 5.1
IRAS 05040+4820 (SAO 40039).........	2,447,919			3.16 ± 0.14	141.9 ± 1.2	3.61 ± 0.05	141.0 ± 0.4	3.55 ± 0.05	139.2 ± 0.4	3.34 ± 0.12	139.0 ± 1.0
	2,448,926			3.31 ± 0.53	139 ± 5	3.15 ± 0.17	139 ± 2	3.42 ± 0.12	144 ± 1	3.13 ± 0.21	147 ± 2
IRAS 06338+5333 (HD 46703)	2,447,919			1.04 ± 0.11	52.1 ± 3.0	0.62 ± 0.05	44.9 ± 2.4	0.56 ± 0.05	47.1 ± 2.4	0.42 ± 0.11	55.6 ± 7.5
IRAS 07008+1050 (HD 52961)	2,448,336			0.96 ± 0.17	13.2 ± 5.0	1.37 ± 0.07	7.6 ± 1.5	1.03 ± 0.06	0.1 ± 1.7	0.83 ± 0.11	171.2 ± 3.9
IRAS 07134+1005 (HD 56126)	2,447,811			0.11 ± 0.10	134.9 ± 23.4	0.35 ± 0.03	43.5 ± 2.7	0.12 ± 0.03	46.6 ± 6.9	0.18 ± 0.06	94.5 ± 9.6
	2,447,811			0.26 ± 0.07	70 ± 5.6	0.22 ± 0.03	56.1 ± 3.0	0.15 ± 0.03	59.3 ± 3.9		
	2,447,823			0.28 ± 0.07	48.5 ± 7.2	0.16 ± 0.03	78.1 ± 6.1	0.21 ± 0.03	63.0 ± 4.3	0.11 ± 0.05	65.7 ± 14.0
	2,447,823			0.24 ± 0.07	102.2 ± 8.8	0.27 ± 0.03	48.9 ± 3.5	0.08 ± 0.03	40.9 ± 9.6		
	2,447,919			0.19 ± 0.09	124.3 ± 13.7	0.04 ± 0.04	31.3 ± 28.1	0.25 ± 0.03	53.0 ± 3.6	0.34 ± 0.06	56.3 ± 5.4
	2,448,237			0.69 ± 0.17	158.3 ± 7.0	0.18 ± 0.06	71.0 ± 9.0	0.15 ± 0.05	179.3 ± 9.1	0.32 ± 0.09	179.0 ± 8.0
IRAS 07331+0021 (AI CMi)	2,447,919	3.82 ± 2.09	53.0 ± 15.6	3.75 ± 0.15	78.4 ± 1.2	2.51 ± 0.04	77.5 ± 0.4	1.62 ± 0.02	81.4 ± 0.4	1.12 ± 0.05	78.8 ± 1.2
	2,447,970	9.54 ± 2.67	138.1 ± 7.8	3.05 ± 0.15	64.2 ± 1.4	1.59 ± 0.05	57.6 ± 1.0	0.84 ± 0.03	59.6 ± 0.9	0.65 ± 0.05	46.1 ± 2.2
	2,448,599			1.03 ± 0.52	136 ± 21	0.21 ± 0.27	161 ± 55	0.34 ± 0.18	131 ± 22		
	2,448,648			1.59 ± 0.35	11 ± 6	2.53 ± 0.11	174 ± 1	1.62 ± 0.05	176 ± 1		
	2,448,713			2.63 ± 0.45	33 ± 5	1.83 ± 0.13	19 ± 2	1.34 ± 0.04	11 ± 1		
	2,449,016			1.85 ± 0.35	39 ± 6	1.05 ± 0.08	16 ± 2	0.90 ± 0.05	5 ± 2	0.90 ± 0.07	00 ± 2
IRAS 07559−5859 (HD 65750)...........	2,447,920			2.74 ± 0.15	86.9 ± 1.6	1.67 ± 0.06	96.6 ± 1.0	1.65 ± 0.07	94.5 ± 1.1	1.61 ± 0.07	101.9 ± 1.2
IRAS 10215−5916											
(HD 302821; CPD −58°2154).........	2,447,919			4.10 ± 0.26	108.4 ± 1.8	4.30 ± 0.09	103.5 ± 0.6	4.36 ± 0.07	108.5 ± 0.5	3.99 ± 0.08	107.6 ± 0.5
	2,448,650			3.60 ± 0.35	132 ± 3	4.19 ± 0.15	126 ± 1	3.94 ± 0.20	128 ± 2		
IRAS 11000−6153 (HD 95767)...........	2,447,919			2.14 ± 0.18	119.4 ± 2.5	1.56 ± 0.09	115.1 ± 1.6	2.12 ± 0.10	115.9 ± 1.3	1.71 ± 0.13	126.1 ± 2.2
IRAS 11331−1418 (HD 100764).........	2,447,971			0.13 ± 0.12	127.2 ± 25.1	0.20 ± 0.05	74.9 ± 6.7	0.01 ± 0.04	102.6 ± 6.0	0.40 ± 0.08	78.0 ± 5.5
	2,448,398					0.42 ± 0.14	26.3 ± 9.2				
IRAS 11385−5517 (HD 101584).........	2,447,919			0.96 ± 0.06	119.0 ± 1.8	1.36 ± 0.04	118.6 ± 0.9	1.33 ± 0.05	116.3 ± 1.1	1.31 ± 0.06	122.5 ± 1.3
	2,448,237			1.31 ± 0.16	113.1 ± 3.6	1.41 ± 0.16	99.4 ± 3.1	1.90 ± 0.11	125.4 ± 1.6		
	2,448,305			1.21 ± 0.16	116.5 ± 3.6	1.60 ± 0.10	115.5 ± 1.8	2.01 ± 0.09	114.8 ± 1.3	1.92 ± 0.11	117.9 ± 1.6
	2,448,398			1.51 ± 0.19	117.5 ± 4.7	1.64 ± 0.12	109.3 ± 2.0	1.22 ± 0.10	120.2 ± 2.4	1.46 ± 0.15	110 ± 3
IRAS 12175−5338											
(SAO 239853; CPD −53°5072)	2,447,919					0.90 ± 0.10	73.5 ± 3.0	0.56 ± 0.11	79.5 ± 5.5	2.38 ± 0.29	58.4 ± 3.4
	2,447,971			1.05 ± 0.15	85.2 ± 4.1	0.82 ± 0.07	70.2 ± 2.4	1.36 ± 0.06	70.0 ± 1.4	1.83 ± 0.15	67.2 ± 2.4
	2,448,399			5.32 ± 1.31	60.6 ± 7.0	3.61 ± 0.30	56.2 ± 2.4				
	2,448,650			2.08 ± 0.46	10 ± 6	0.16 ± 0.24	134 ± 43	0.74 ± 0.26	61 ± 10		
IRAS 12222−4652 (HD 108015).........	2,447,920			0.97 ± 0.07	177 ± 2	0.55 ± 0.04	176.1 ± 2.3	0.44 ± 0.04	175.6 ± 2.5	0.14 ± 0.07	16.6 ± 14
	2,448,398			0.91 ± 0.22	2.8 ± 7.0	1.17 ± 0.12	164 ± 2.8	0.33 ± 0.09	153 ± 8.3	1.35 ± 0.20	165.2 ± 4.2
IRAS 12538−2611 (HR 4912)	2,447,920			0.36 ± 0.08	147.9 ± 6.7	0.18 ± 0.03	103.6 ± 4.6	0.18 ± 0.03	92.4 ± 4.4	0.34 ± 0.04	85.0 ± 3.5
	2,448,743					0.40 ± 0.10	151 ± 7	0.30 ± 0.06	67 ± 6	0.44 ± 0.09	141 ± 6
IRAS 15039−4806 (HD 133656).........	2,447,920					0.37 ± 0.07	87.4 ± 5.4				
	2,448,307			0.27 ± 0.17	89.6 ± 13	0.39 ± 0.09	76.3 ± 6.8	0.31 ± 0.07	118.8 ± 6.0	0.16 ± 0.10	134.4 ± 20.9
IRAS 16206−5956 (SAO 243756).......	2,448,336					2.26 ± 0.60	81.7 ± 7.5	1.84 ± 0.44	62.3 ± 6.7	0.54 ± 0.72	79.4 ± 37.8
IRAS 17436+5003 (HD 161796)	2,447,682			0.84 ± 0.09	125 ± 3.2	0.72 ± 0.04	109.3 ± 1.7	0.51 ± 0.03	110.6 ± 1.3	0.42 ± 0.03	101.1 ± 1.9
	2,448,336			0.75 ± 0.13	104.2 ± 4.8	0.86 ± 0.06	110.8 ± 1.9	0.72 ± 0.04	111.5 ± 1.8	0.82 ± 0.11	105.9 ± 3.8
	2,448,399			0.88 ± 0.09	111.6 ± 3.1	0.78 ± 0.05	109.3 ± 2	0.66 ± 0.10	110 ± 4.5	0.75 ± 0.09	118.9 ± 3.6

TABLE 2—*Continued*

		U		B		V		R		I	
Object	Date (JD)	P (%)	θ (deg)	P (%)	θ (deg)	P (%)	θ (deg)	P (%)	θ (deg)	P (%)	θ (deg)
IRAS 17534+2603											
(HD 163506; 89 Her)	2,447,659	1.19 ± 0.12	67 ± 2	0.77 ± 0.03	60 ± 0.7	0.61 ± 0.02	66 ± 0.5	0.44 ± 0.02	66 ± 0.7	0.51 ± 0.03	65 ± 0.8
	2,447,659	1.01 ± 0.08	49 ± 2	0.67 ± 0.06	49 ± 1.6	0.60 ± 0.02	68 ± 0.6				
	2,447,682			1.23 ± 0.06	76 ± 1.4	0.83 ± 0.02	76.7 ± 0.8	0.54 ± 0.02	76.8 ± 0.8	0.57 ± 0.02	72.7 ± 1.1
	2,448,307	1.10 ± 0.18	76.5 ± 4.8	0.89 ± 0.07	80.7 ± 2.4	0.79 ± 0.05	92.9 ± 1.7	0.87 ± 0.04	100.1 ± 1.2	0.69 ± 0.06	105.9 ± 2.6
	2,448,399			0.88 ± 0.05	89.7 ± 1.6	0.70 ± 0.03	81.0 ± 1.3	0.59 ± 0.03	94.1 ± 1.4	0.35 ± 0.05	94.6 ± 4.0
IRAS 18095+2704	2,448,370			7.06 ± 0.58	127.2 ± 2.3	6.68 ± 0.21	128.3 ± 0.9	4.94 ± 0.11	126.1 ± 0.7	4.08 ± 0.28	124.7 ± 1.9
IRAS 18184−1623 (HD 168625)	2,448,306			4.44 ± 0.40	13.7 ± 2.6	3.97 ± 0.16	12.3 ± 1.1	3.75 ± 0.09	12.1 ± 0.7	4.12 ± 0.18	11.0 ± 1.3
	2,448,370			1.83 ± 0.27	32.7 ± 4.2	2.19 ± 0.08	24.0 ± 1.1	1.70 ± 0.05	20.4 ± 0.8	1.33 ± 0.08	24.9 ± 1.7
IRAS 19114+0002 (HD 179821)	2,447,683			2.04 ± 0.24	58.8 ± 3.4	1.95 ± 0.05	47.7 ± 0.7	0.96 ± 0.02	46.5 ± 0.6	0.82 ± 0.02	53.7 ± 0.7
	2,447,824					1.96 ± 0.03	45.2 ± 0.4	1.55 ± 0.03	51.5 ± 0.5		
IRAS 19114+0002 (HD 179821)	2,448,336			2.4 ± 0.42	35.6 ± 5.0	2.15 ± 0.09	43.4 ± 1.2	2.56 ± 0.26	37.4 ± 2.9	1.16 ± 0.13	00.0 ± 3.2
	2,448,399			2.56 ± 0.23	42.4 ± 2.6	1.93 ± 0.07	41.3 ± 1.1	1.44 ± 0.04	42.2 ± 0.9	1.16 ± 0.08	48.8 ± 1.9
IRAS 19486+1350 (TW Aql)	2,448,397			0.39 ± 0.70	114.4 ± 51.6	0.89 ± 0.40	97.7 ± 13	0.38 ± 0.31	126.3 ± 23	1.98 ± 1.07	97.4 ± 15.5
IRAS 19500−1709 (HD 187885)	2,447,824					1.58 ± 0.25	161.7 ± 4.5	1.99 ± 0.15	162.3 ± 2.2		
	2,447,826					2.35 ± 0.12	11 ± 1.4				
IRAS 20004+2955 (V1027 Cyg)	2,448,367			1.13 ± 0.59	43.9 ± 14.9			0.82 ± 0.11	8.9 ± 3.9	1.06 ± 0.16	178.2 ± 4
IRAS 22272+5435 (SAO 34504)	2,447,823			3.49 ± 1.38	75.7 ± 11.3	2.28 ± 0.16	47.2 ± 2.0	1.17 ± 0.09	62.4 ± 2.3	1.15 ± 0.20	77.0 ± 4.9
	2,447,823			4.13 ± 1.46	39.6 ± 10.1	1.66 ± 0.15	66.3 ± 2.7	1.12 ± 0.09	57.4 ± 2.2		
	2,447,824					1.07 ± 0.19	52.5 ± 5.0	1.04 ± 0.10	54.7 ± 2.6	1.44 ± 0.21	39.3 ± 4.2

TABLE 3
UBVRI Polarization Measurements of Post-AGB Star HR 4049

Date (JD)	U P (%)	U θ (deg)	B P (%)	B θ (deg)	V P (%)	V θ (deg)	R P (%)	R θ (deg)	I P (%)	I θ (deg)
2,447,918........	0.21 ± 0.09	172 ± 12	0.18 ± 0.03	49 ± 5	0.31 ± 0.03	87 ± 3	0.48 ± 0.03	87 ± 2	0.46 ± 0.05	72 ± 3
2,447,919........			0.21 ± 0.02	56 ± 3	0.33 ± 0.02	76 ± 1	0.35 ± 0.02	76 ± 1	0.33 ± 0.03	86 ± 3
2,447,969........	0.14 ± 0.09	13 ± 17	0.42 ± 0.05	58 ± 3	0.38 ± 0.03	62 ± 3	0.68 ± 0.04	69 ± 2	0.50 ± 0.05	65 ± 3
2,448,236........			0.21 ± 0.06	52 ± 8	0.27 ± 0.06	78 ± 7	0.67 ± 0.05	101 ± 2		
2,448,304........	0.73 ± 0.16	24 ± 6	0.22 ± 0.06	8 ± 8	0.23 ± 0.06	86 ± 8	0.39 ± 0.06	94 ± 4	0.15 ± 0.08	99 ± 15
2,448,397........			0.23 ± 0.05	40 ± 6	0.33 ± 0.04	89 ± 4	0.29 ± 0.05	108 ± 4	0.32 ± 0.06	99 ± 5
2,448,741........					0.35 ± 0.09	63 ± 7	0.25 ± 0.08	59 ± 9	0.44 ± 0.10	104 ± 6

shell with a diameter of 25″. The dust shell has an equatorially enhanced torus inclined at ~60° with respect to the observer.

IRAS 19114+0002 (HD 179821).—Recent detailed studies of this star are not able to establish whether HD 179821 is a low-mass star in the post-AGB stage of evolution or a massive (30 $M_\odot$) yellow supergiant caught in between the red giant branch and Wolf-Rayet phases (Jura & Werner 1999; Reddy & Hrivnak 1999; Thévenin et al. 2000, 2001). Our polarization measurements are in agreement with those of Trammell et al. (1994). Bujarrabal

et al. (1992) mapped this object in CO $J = 2-1$ and $1-0$ and found that the molecular emission is bipolar, with the major axis oriented at an angle of 50° Jura et al. (2001) mapped the CO $J = 1-0$ emission from the circumstellar shell around HD 179821. They found an intrinsically asymmetric circumstellar nebula and proposed that the star will probably explode as a supernova in about 10^5 yr. Gledhill et al. (2001) made high-quality polarimetric imaging observations of HD 179821 in the J, H, and K bands. The extent of the image in total flux in the J, H, and K bands is 7″.2, and
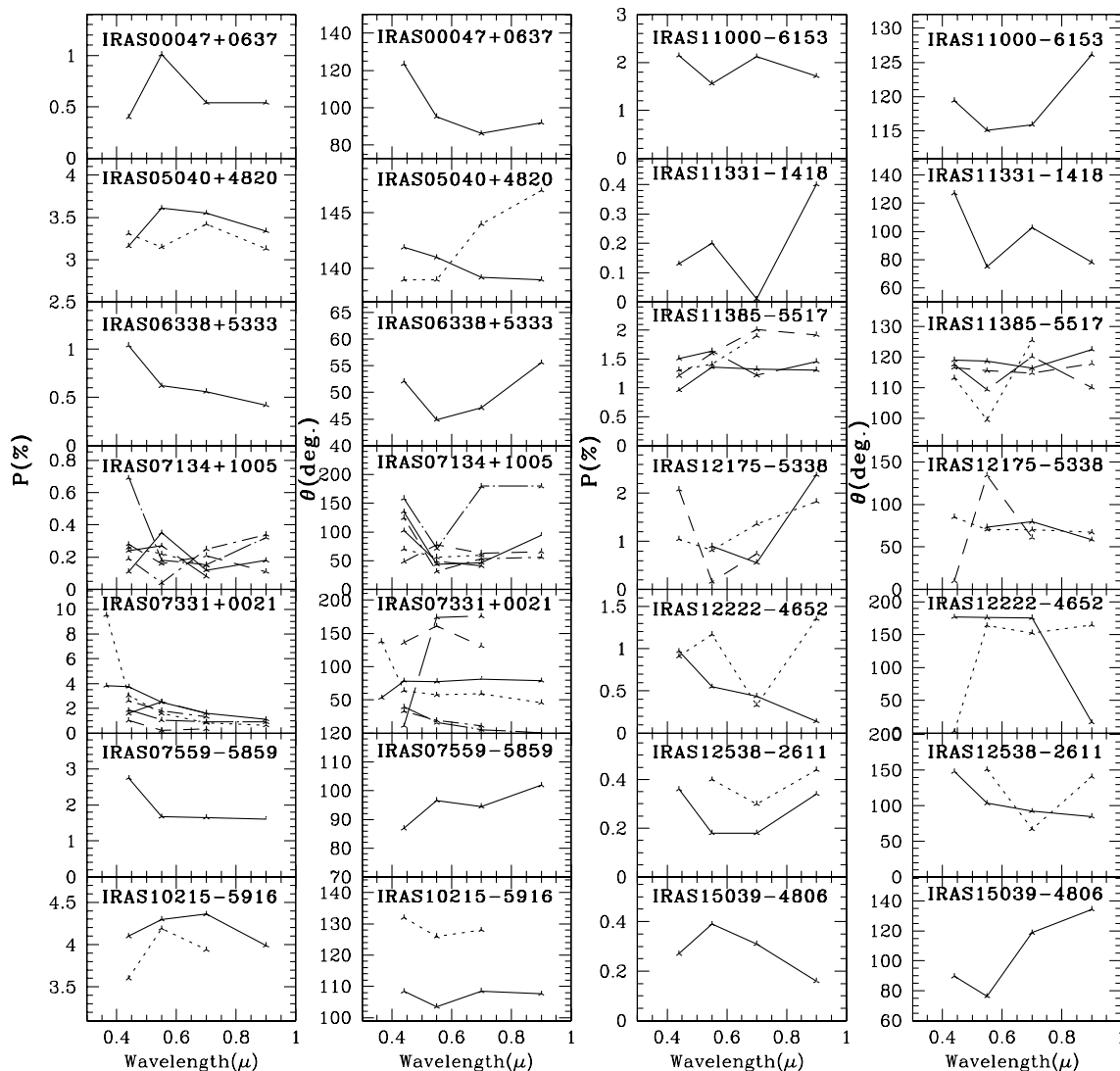

Fig. 1.—*UBVRI* polarization measurements of post-AGB candidates and related stars. P (%) and θ (deg) vs. wavelength for each star are shown side by side.
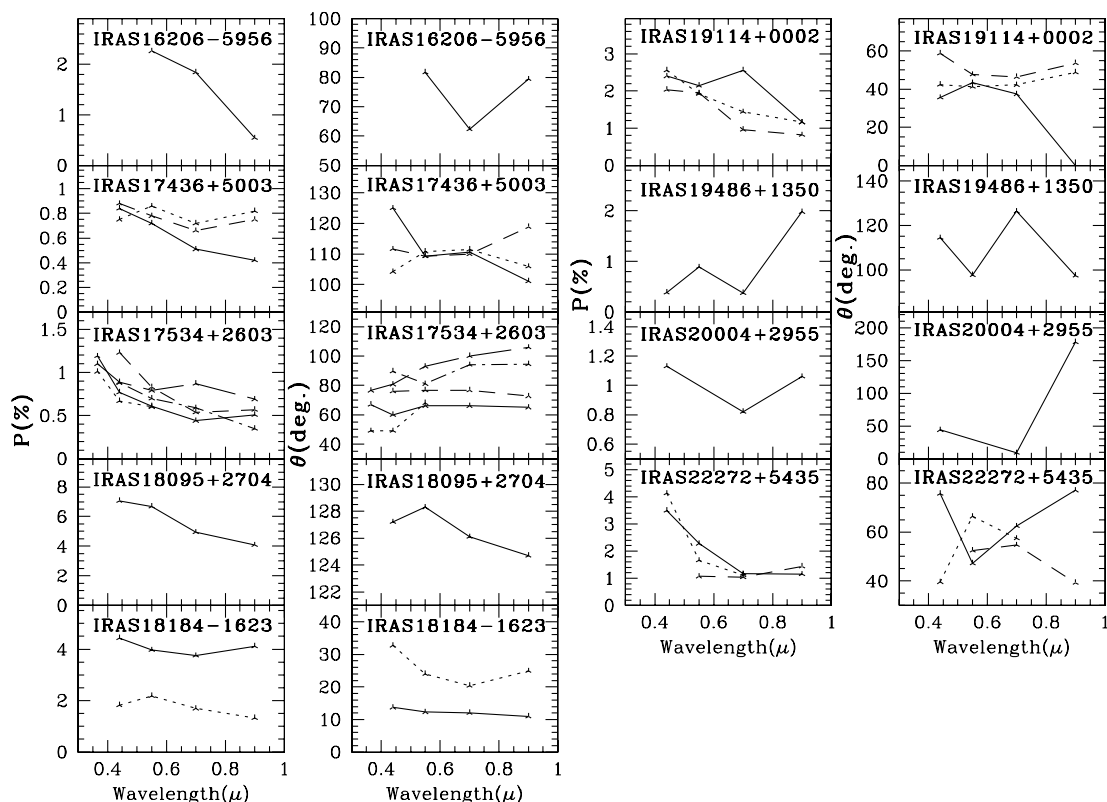
Fig. 1.—*Continued*

polarization is reliably detected out to the full extent of the total-flux image. The *J*, *H*, and *K* polarized flux images show that most of the scattered light originates from a ring of dust surrounding the star. Coronagraphic imaging of HD 179821 by Kastner & Weintraub (1995) detected the extended scattering nebula out to a radius of 9″ in *J* and 6″ in *K*. At a radius of 5″ they measured a polarization of 13% in *J* and 6% in *K*. However, Gledhill et al. (2001) measured a polarization of more than 25% in both *J* and *K* in the outer part of the envelope in their images of HD 179821. Mid-IR imaging of HD 179821 at 12.5 μm (Hawkins et al. 1995) showed a dust ring encircling the star. This ring is very similar to that found in the *J*, *H*, and *K* polarization images of HD 179821 obtained by Gledhill et al. (2001).

In the *HST* WFPC2 image of HD 179821 (Ueta et al. 2000), an extended nebula with a complex structure of concentric shells forming a rosette is revealed. The extent of the nebula in these optical images is similar to that of near-IR images (Gledhill et al. 2001), being approximately 8″ in diameter.

IRAS 19486+1350 (TW Aql).—Parthasarathy & Reddy (1993) classified this as a possible low-mass post-AGB star. It is a yellow semiregular pulsating variable with a period of 64.6 days and observed OH maser emission (Benson & Little-Marenin 1996).

3.2. *Post-AGB Stars with Available HST, Mid-IR, and/or Imaging Polarimetry Observations*

IRAS 07134+1005 (HD 56126).—This is a high Galactic latitude, carbon-rich, post-AGB F supergiant (Hrivnak et al. 1989; Kwok et al. 1989; Parthasarathy et al. 1992) with 21 μm emission. Barthès et al. (2000) found that the central star is variable with a period of 36.8 days. They attributed the spectroscopic and photometric variations of the star to radial pulsations that yield shock waves that propagate through the atmosphere and generate a complex asynchronous motion in the outer hydrogen layers.

We have made *BVRI* polarization measurements on four different dates. The data indicate variable intrinsic polarization. *HST* WFPC2 images of HD 56126 revealed large (>4″), faint nebulosity (Ueta et al. 2000). The size of the optical reflection nebulosity in IRAS 07134+1005 (HD 56126) is the largest among the post-AGB stars with 21 μm emission and is comparable to that in mid-IR images (Meixner et al. 1997; Jura et al. 2000). CO *J* = 1−0 emission arising in the circumstellar envelope of the object was found to extend from 1″.2 to 7″ in radius from the central star (Meixner et al. 2004). Using NICMOS on *HST*, Ueta et al. (2004, 2005) performed imaging polarimetry of HD 56126 and concluded that it has an equatorially enhanced, prolate hollow spheroidal shell that is nearly edge-on.

IRAS 17436+5003 (HD 161796).—Polarization observations of the post-AGB star HD 161796 (Parthasarathy & Pottasch 1986) were also made by Joshi et al. (1987), Nook (1993), Trammell et al. (1994), and Gledhill et al. (2001). Joshi et al. (1987) and Nook (1993) found evidence for intrinsic polarization. However, Trammell et al. (1994) concluded that the observed polarization is interstellar. Gledhill et al. (2001) found high degrees of polarization in both the *J* and *K* bands forming an almost perfect centrosymmetric pattern, indicating scattering in an optically thin medium with a point source illuminator. We made polarization measurements on three different occasions. Our polarization measurements indicate intrinsic polarization. Gledhill et al. (2001) observations show the similarity of the polarimetry in the *J* and *K* bands, implying that small dust grains are responsible for scattering the light and that the scattering geometry is very similar in *J* and *K*. They find that the polarization pattern extends more in the north-south direction than in the east-west direction, suggesting that the reflection nebula is slightly elongated. In *HST* WFPC2 imaging observations (Ueta et al. 2000), IRAS 17436+5003 appears as an elliptical nebula at optical wavelengths, similar

to that found by Gledhill et al. (2001) in the near-IR data. The IR imaging at 10.5 and 12.5 μm (Skinner 1994) revealed a dusty torus oriented perpendicular to the major axis of the optical (Ueta et al. 2000) and near-IR emission (Gledhill et al. 2001). They estimated an inner radius of 0″.48 for this torus. This agrees remarkably well with the 0″.6 inner radius of the shell seen in the polarized flux images in J and K (Gledhill et al. 2001). It seems highly likely, therefore, that the dust "torus" seen in emission by Skinner et al. is also responsible for scattering much of the light in our $BVRI$ polarization data and in the J- and K-band imaging polarimetry data of Gledhill et al. (2001). The observations of Gledhill et al. (2001) indicate an optically thin, ellipsoidal shell of dust with an equatorial density enhancement, and the sharpness of the inner edge of the shell (Fig. 3 in Gledhill et al. 2001) indicates that it is physically detached from the star and that the interior is relatively empty of dust.

IRAS 18095+2704.—This is a high Galactic latitude, F-type post-AGB star (Hrivnak et al. 1989). Our polarization measurements are in good agreement with those of Trammell et al. (1994) and Gledhill et al. (2001) and clearly show the presence of intrinsic polarization similar to that of IRAS 04296+3429 (Trammell et al. 1994). The interstellar polarization for IRAS 18095+2704 was estimated by Trammell et al. (1994). The J and K polarization maps indicate that scattering is indeed occurring and that IRAS 18095+2704 has an extended envelope forming a reflection nebula at near-IR wavelengths. The polarized flux images in J and K (Gledhill et al. 2001) reveal a bipolar geometry for the scattered light in IRAS 18095+2704. The WFPC2 V- and I-band images of Ueta et al. (2000) show a bipolar nebula and indicate that there is a dusty disk or torus surrounding the star that is responsible for collimating the outflow into two bipolar lobes. The aligned vectors in the polarization patterns in J and K indicate that dust grains in the bipolar lobes do not have a direct view of the source and that multiple scattering is important (Gledhill et al. 2001). Our polarization data show a higher percent of polarization toward shorter wavelengths, indicating that the star is more obscured at shorter wavelengths.

IRAS 19500−1709 (HD 187885).— This is a high Galactic latitude carbon-rich post-AGB F supergiant (Parthasarathy et al. 1988; van Winckel 2003). Gledhill et al. (2001) performed imaging polarimetry of this object in the J and K bands. The J and K polarization maps show that the star illuminates a reflection nebula that extends to a radius of more than 2″ in the J band. The polarizations are higher along an east-west axis than along a north-south axis. Gledhill et al. (2001) find evidence in their polarization maps that the vectors are oriented preferentially north-south in the core region, suggesting that multiple scattering is occurring in this region. The J-band polarized flux image clearly shows that the illumination is indeed anisotropic and that HD 187885 (IRAS 19500−1709) is a bipolar nebula in scattered light. Gledhill et al. (2001) find similar results from the K-band polarization map and conclude that this object is intrinsically polarized and appears as a bipolar reflection nebula in the near-IR. Recently, based on images obtained with the mid-IR camera OSCIR mounted on the Gemini North Telescope, Clube & Gledhill (2004) have also suggested an optically thin, detached axisymmetric dust shell surrounding the central star.

IRAS 22272+5435 (SAO 34504).—Our polarization measurements of this object clearly show the presence of variable intrinsic polarization, and the percentage of polarization is found to be higher in the blue, indicating scattering. Trammell et al. (1994) also find evidence for the presence of intrinsic polarization. In the J-band polarization map, Gledhill et al. (2001) find that it is centrosymmetric, indicating that the star illuminates an
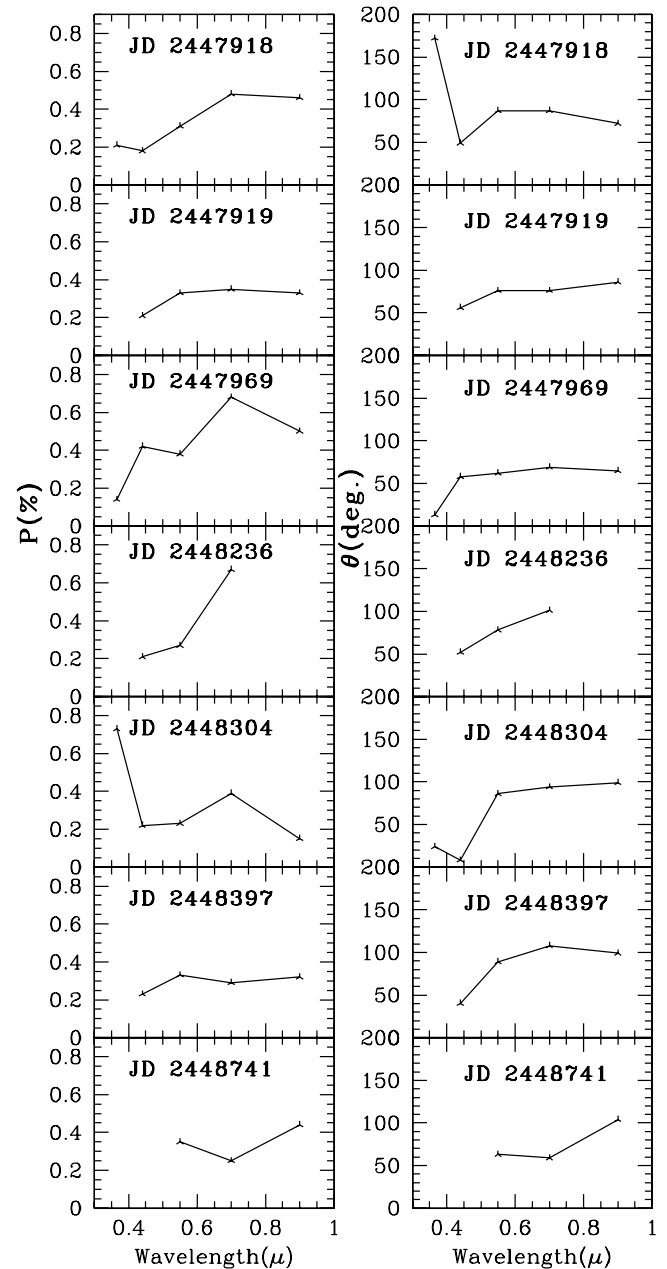

Fig. 2.—Our polarization measurements of HR 4049.

extended reflection nebula and that the illumination is isotropic, similar to that of HD 161796. The mid-IR images (Meixner et al. 1999) and optical *HST* WFPC2 images (Ueta et al. 2000) also show similar results. In the polarized flux image, Gledhill et al. (2001) found a ringlike structure and suggested that the polarized flux ring corresponds to a shell of dust around the star, where most of the scattering is taking place. In mid-IR images of the object (Ueta et al. 2001), the dust shell was found to have a toroidal structure with a 0″.5 inner radius.

3.3. *IRAS 10158−2844 (HR 4049)*

HR 4049 is a high Galactic latitude, extremely metal-poor ([Fe/H] $= -4.8$; Waelkens et al. 1991b; Takeda et al. 2002) post-AGB star. It shows light and radial velocity variations with a period near 430 days (Waelkens et al. 1991a; van Winckel et al. 1995).

We have made polarization measurements of HR 4049 several times (Table 3; Fig. 2). The polarization is time-variable.

TABLE 4
POLARIZATION MEASUREMENTS OF HR 4049 COLLECTED FROM THE LITERATURE

DATE (JD)	U P (%)	U θ (deg)	B P (%)	B θ (deg)	V P (%)	V θ (deg)	R P (%)	R θ (deg)	I P (%)	I θ (deg)	REFERENCES
2,446,505.............	0.39 ± 0.11	179 ± 8	0.30 ± 0.04	34 ± 4	0.33 ± 0.03	66 ± 3	0.45 ± 0.10	59 ± 6			1
2,447,648.............	0.66 ± 0.05	15.6 ± 2.2	0.33 ± 0.03	30.6 ± 2.6	0.28 ± 0.03	50 ± 3	0.29 ± 0.03	52 ± 3	0.26 ± 0.03	54 ± 3	2
2,447,602.............	0.47 ± 0.07	15.4	0.34 ± 0.01	31.1	0.29 ± 0.01	47.7	0.27 ± 0.01	49.4			3
2,447,927.............	0.58 ± 0.11	5.7	0.29 ± 0.004	43.2	0.34 ± 0.003	59.0	0.34 ± 0.004	52.4			3
2,447,934.............	0.13 ± 0.13	53.2	0.27 ± 0.007	40.7	0.29 ± 0.006	61.2	0.33 ± 0.008	63.9			3
2,447,948.............	0.43	18.1	0.30	49.0	0.33	63.1	0.37	65.9			3
2,447,989.............	0.59	8.8	0.27	44.9	0.34	61.2	0.32	64.0			3
1993 Jan...............					0.51 ± 0.2	60 ± 5					4

REFERENCES.—(1) Joshi et al. 1987; (2) Johnson & Jones 1991; (3) Nook 1993; (4) Trammel et al. 1994.
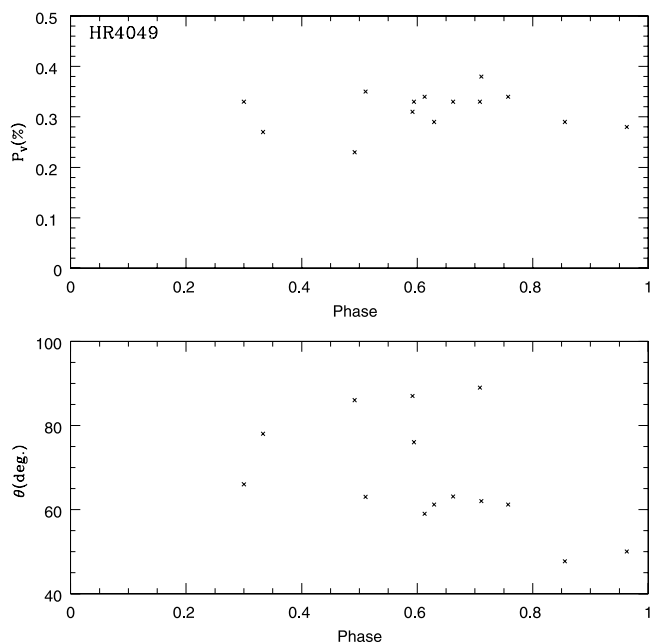
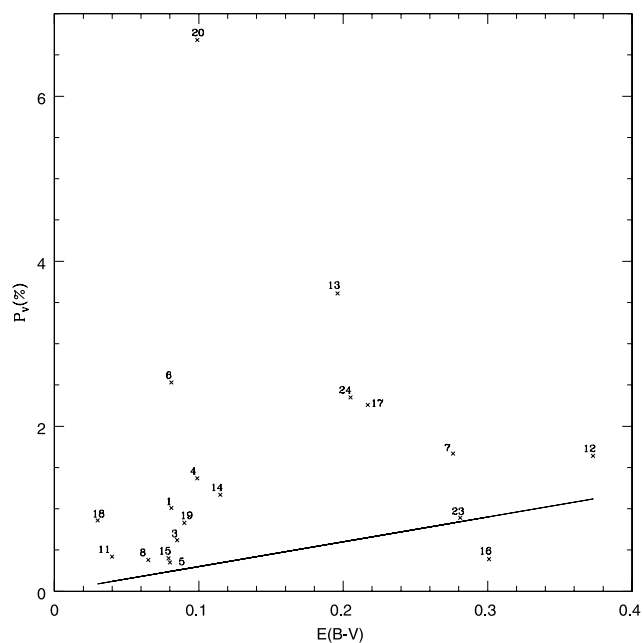Fig. 3.—Percentage polarization and angle vs. orbital phases of HR 4049.

Fig. 4.—Maximum observed V-band percentage polarization for the stars vs. interstellar $E(B - V)$. The solid line represents the mean interstellar polarization, $P_V = 3E(B - V)$.

Combining our measurements with those of Joshi et al. (1987), Johnson & Jones (1991), Nook (1993), and Trammell et al. (1994) (Table 4), we plotted the variation of polarization and position angle with the orbital phase (Fig. 3). The small degree of polarizations observed may indicate a spherically symmetric dust envelope. Furthermore, although we find a variation in the position angle of polarization with the orbital phase of the system, Figure 3 does not establish a definite relationship between the two. This is in contrast to the conclusions of Johnson et al. (1999). They formulated the hypothesis that HR 4049 is surrounded by an optically thin, spherical, circumbinary disk and that the orientation of the disk is tied to the orbit of the binary. This seemed consistent with the observation that the circumstellar extinction in the case of HR 4049 was found to vary with the orbital phase (Waelkens et al. 1991a; Monier & Parthasarathy 1999). Waelkens et al. (1991a) suggested that during the light minimum of the binary system, some of the small and hot dust particles are converted to larger and cooler ones. Such variations in the circumstellar matter surrounding the central star may explain the observed extinction variations. Recently, based on VINCI-VLTI observations, Antoniucci et al. (2005) have been favoring a more spherical envelope around HR 4049, as opposed to a circumbinary disk model as proposed by earlier authors. However, owing to the limited spatial frequency covered, they are not able to exclude the circumbinary disk model. Our polarization data, the observations of Antoniucci et al. (2005), and those of earlier authors suggest that HR 4049 may have a multistructured envelope

4. DISCUSSION AND CONCLUSIONS

Nineteen stars in our sample have $|b| > 5°$. Using the *IRAS* DIRBE dust maps (Schlegel et al. 1998) we estimated the interstellar extinction $[E(B - V)]$ in the direction of these stars (Table 1). The *IRAS* DIRBE dust maps do not give reliable estimates of the interstellar extinction for $|b| < 5°$. The *IRAS* DIRBE

reddening estimates have an accuracy of 16%. The mean ratio of interstellar polarization to reddening is $P_V/E(B - V) = 3\%$ mag^{-1}. Many stars in our list show variable polarization. In Figure 4 we have plotted the maximum observed V-band polarization of the stars (P_V) against interstellar reddening $E(B - V)$ along with the mean interstellar polarization $[P_V = 3E(B - V)]$. We find that the maximum observed V-band polarization is greater than the mean interstellar contribution to the polarization in the case of 18 stars, indicating that those stars are intrinsically polarized. IRAS 15039−4806 (HD 133656) lies below the mean interstellar polarization curve.

Several stars given in Table 2 exhibit polarization properties that indicate large-scale asphericity. They show $P(\lambda)$ curves (Fig. 1) that rise very rapidly to the blue and gradual position angle rotations with wavelength, e.g., IRAS 18095+2704. Such position angle rotations indicate the presence of two polarization sources. In the case of some of the objects, the steep $P(\lambda)$ dependence and large degree of polarization cannot be explained by interstellar polarization and suggest that the polarization mechanism in the blue is scattering.

Several objects show time-variable polarizations. The $P(\lambda)$ curves are not matched well by a Serkowski law, and time variability of the polarization indicates that the observed polarization is intrinsic. These objects are IRAS 07134+1005 (HD 56126), IRAS 07331+0021 (AI CMi), IRAS 12538−2611 (HR 4912), IRAS 10158−2844 (HR 4049), IRAS 10215−5916 (CPD −58°2154), IRAS 17534+2603 (89 Her), IRAS 19114+0002 (HD 179821), and IRAS 22272+5435 (HD 235858). The binary nature of some of these objects, on going post-AGB mass loss, and the pulsations common in post-AGB stars may cause variations in the circumstellar environments of these stars, leading to variations in the observed polarizations.

REFERENCES

Antoniucci, S., Paresce, F., & Wittkowski, M. 2005, A&A, 429, L1
Barthès, D., Lèbre, A., Gillet, D., & Mauron, N. 2000, A&A, 359, 168
Benson, P. J., & Little-Marenin, I. R. 1996, ApJS, 106, 579
Bujarrabal, V., Alcolea, J., & Planesas, P. 1992, A&A, 257, 701

Chiar, J. E., Whittet, D. C. B., & Aitken, D. K. 1993, ApJ, 409, 404
Clube, K. L., & Gledhill, T. M. 2004, in ASP Conf. Ser. 313, Asymmetrical Planetary Nebulae III: Winds, Structure, and the Thunderbird, ed. M. Meixner et al. (San Francisco: ASP), 359

Fernie, J. D. 1974, PASP, 86, 837

Gledhill, T. M., Chrysostomou, A., Hough, J. H., & Yates, J. A. 2001, MNRAS, 322, 321

Hawkins, G. W., Skinner, C. J., Meixner, M. M., Jernigan, J. G., Arens, J. F., Keto, E., & Graham, J. R. 1995, ApJ, 452, 314

Hrivnak, B. J., Kwok, S., & Volk, K. M. 1989, ApJ, 346, 265

Hsu, J., & Breger, M. 1982, ApJ, 262, 732

Hutsemekers, D., Van Drom, E., Gosset, E., & Melnick, J. 1994, A&A, 290, 906

Jain, S. K., & Srinivasulu, G. 1991, Opt. Eng., 30, 1415

Johnson, J. J., & Jones, T. J. 1991, AJ, 101, 1735

Johnson, J. J., et al. 1999, MNRAS, 306, 531

Joshi, U. C., Deshpande, M. R., Sen, A., & Kulshrestha, A. 1987, A&A, 181, 31

Jura, M., Chen, C., & Werner, M. W. 2000, ApJ, 544, L141

Jura, M., Velusamy, T., & Werner, M. W. 2001, ApJ, 556, 408

Jura, M., & Werner, M. W. 1999, ApJ, 525, L113

Kastner, J. H., & Weintraub, D. A. 1995, ApJ, 452, 833

Kwok, S. 1993, ARA&A, 31, 63

Kwok, S., Volk, K., & Hrivnak, B. J. 1989, ApJ, 345, L51

Meixner, M. 2000, in ASP Conf. Ser. 199, Asymmetrical Planetary Nebulae II: From Origins to Microstructures, ed. J. H. Kastner et al. (San Francisco: ASP), 135

Meixner, M., Skinner, C. J., Graham, J. R., Keto, E., Jernigan, J. G., & Arens, J. F. 1997, ApJ, 482, 897

Meixner, M., Zalucha, A., Ueta, T., Fong, D., & Justtanont, K. 2004, ApJ, 614, 371

Meixner, M., et al. 1999, ApJS, 122, 221

Molster, F. J., et al. 1999, A&A, 350, 163

Monier, R., & Parthasarathy, M. 1999, A&A, 341, 117

Nook, M. A. 1993, in ASP Conf. Ser. 45, Luminous High-Latitude Stars, ed. D. D. Sasselov (San Francisco: ASP), 1993

O'Hara, T. B., Meixner, M., Speck, A. K., Ueta, T., & Bobrowsky, M. 2003, ApJ, 598, 1255

Parthasarathy, M. 1989, in IAU Colloq. 106, Evolution of Peculiar Red Giant Stars, ed. H. R. Johnson & B. Zuckerman (Cambridge: Cambridge Univ. Press), 384

———. 1991, A&A, 247, 429

Parthasarathy, M., García-Lario, P., & Pottasch, S. R. 1992, A&A, 264, 159

Parthasarathy, M., & Jain, S. K. 1993, in IAU Symp. 155, Planetary Nebulae, ed. R. Weinberger & A. Acker (Dordrecht: Kluwer), 353

Parthasarathy, M., & Pottasch, S. R. 1986, A&A, 154, L16

Parthasarathy, M., Pottasch, S. R., & Wamsteker, W. 1988, A&A, 203, 117

Parthasarathy, M., & Reddy, B. E. 1993, Bull. Astron. Soc. India, 21, 619

Parthasarathy, M., Vijapurkar, J., & Drilling, J. S. 2000, A&AS, 145, 269

Pottasch, S. R., & Parthasarathy, M. 1988, A&A, 192, 182

Reddy, B. E., & Hrivnak, B. J. 1999, AJ, 117, 1834

Robberto, M., & Herbst, T. M. 1998, ApJ, 498, 400

Schlegel, D. J., Finkbeiner, D. P., & Davis, M. 1998, ApJ, 500, 525

Serkowski, K., Mathewson, D. S., & Ford, V. L. 1975, ApJ, 196, 261

Sivarani, T., Parthasarathy, M., García-Lario, P., & Manchado, A. 2001, in Post-AGB Objects as a Phase of Stellar Evolution, ed. R. Szczerba & S. K. Gorny (Dordrecht: Kluwer), 305

Skinner, C. J. 1994, MNRAS, 271, 300

Sterken, C., Arentoft, T., Duerbeck, H. W., & Brogt, E. 1999, A&A, 349, 532

Takeda, Y., et al. 2002, Publ. Astron. Soc. Japan, 54, 765

Thévenin, F., Jasniewicz, G., & Parthasarathy, M. 2001, in Post-AGB Objects as a Phase of Stellar Evolution, ed. R. Szczerba & S. K. Gorny (Dordrecht: Kluwer), 313

Thévenin, F., Parthasarathy, M., & Jasniewicz, G. 2000, A&A, 359, 138

Trammell, S. R., Dinerstein, H. L., & Goodrich, R. W. 1994, AJ, 108, 984

Ueta, T., Meixner, M., & Bobrowsky, M. 2000, ApJ, 528, 861

Ueta, T., Murakawa, K., & Meixner, M. 2004, in ASP Conf. Ser. 313, Asymmetrical Planetary Nebulae III: Winds, Structure, and the Thunderbird, ed. M. Meixner et al. (San Francisco: ASP), 38

———. 2005, AJ, 129, 1625

Ueta, T., et al. 2001, ApJ, 557, 831

van Winckel, H. 2003, ARA&A, 41, 391

van Winckel, H., Waelkens, C., & Waters, L. B. F. M. 1995, A&A, 293, L25

Waelkens, C., Lamers, H. J. G. L. M., Waters, L. B. F. M., Rufener, F., Trams, N. R., La Bertre, T., Ferlet, R., & Vidal-Madjar, A. 1991a, A&A, 242, 433

Waelkens, C., van Winckel, H., Bogaert, E., & Trams, N. R. 1991b, A&A, 251, 495

Whitelock, P., Menzies, J. W., Catchpole, R. M., Feast, M. W., Carter, B. S., Marang, F., Roberts, G., & Sekiguci, K. 1989, MNRAS, 241, 393

Wilking, B. A., Lebofsky, M. J., Kemp, J. C., Martin, P. G., & Rieke, G. H. 1980, ApJ, 235, 905